NATIONAL ADVISORY COMMITTEE FOR AERONAUTICS

WARTIME REPORT

ORIGINALLY ISSUED

February 1945 as
Memorandum Report E5B23

FLIGHT AND TEST- STAND INVESTIGATION OF HIGH-PERFORMANCE FUELS

IN DOUBLE-ROW RADIAL AIR-COOLED ENGINES

III - COMPARISON OF COOLING CHACTERISTICS OF

FLIGHT AND TEST-STAND ENGINES

By H. Jack White, Calvin C. Blackman, and Marcel Dandois

Aircraft Engine Research Laboratory
Cleveland, Ohio

NACA

WASHINGTON

NATIONAL ADVISORY COMMITTEE FOR AERONAUTICS

<u>MEMORANDUM REPORT</u>

for the

Army Air Forces, Air Technical Service Command

FLIGHT AND TEST-STAND INVESTIGATION OF HIGH-PERFORMANCE FUELS

IN DOUBLE-ROW RADIAL AIR-COOLED ENGINES

III - COMPARISON OF COOLING CHARACTERISTICS OF

FLIGHT AND TEST-STAND ENGINES

By H. Jack White, Calvin C. Blackman, and Marcel Dandois

SUMMARY

The cooling characteristics of 14-cylinder double-row radial air-cooled engines have been compared in a test stand and in flight. The three types of NACA cooling tests were made for both engines: variable charge-air flow, variable cooling-air pressure drop, and variable fuel-air ratio. Test-stand runs were made at ground-level atmospheric conditions; flight tests were conducted in a four-engine airplane in a single flight at a pressure altitude of 7000 feet. All tests were made at an engine speed of approximately 2230 rpm, in low blower ratio, and with normal spark advance for these engines (25° B.T.C.).

For the same operating conditions, the test-stand engine was found to run consistently cooler than the flight engine. Estimates of temperature-limited engine performance, based on cooling-air pressure drops experienced with the airplane, indicate that both engines may be expected to satisfy the temperature limits specified by the engine manufacturer for the rear-spark-plug gasket at various power ratings. Based both on similar estimates and on actual temperatures obtained in flight during conventional operation of the test engine, a maximum rear middle-barrel temperature of 350° F, which corresponds approximately to the manufacturer's maximum cylinder rear-hold-down-flange temperature of 335° F, will probably be exceeded by either engine at take-off power. At lower power levels this temperature

limit will probably be exceeded by the flight engine at all conditions and may be exceeded by the test-stand engine at some conditions.

INTRODUCTION

At the request of the Army Air Forces, Air Technical Service Command, an investigation is being conducted at the Cleveland laboratory of the NACA to evaluate triptane in relation to other high-antiknock fuel components as a blending agent for aviation fuels. This paper is the third in a series of reports that present fuel-knock and engine-cooling data with double-row radial air-cooled multicylinder engines. This investigation conducted during the summer of 1944, includes tests with engine installations in a test stand and in flight.

In order that fuel knock limits could be compared with the cooling limits of the double-row radial air-cooled engine, as installed in the airplane, the cooling characteristics were studied and are reported in part I (reference 1). A presentation of all the knock data for 28-R fuel, a blend of triptane and 28-R, and a blend of xylidines and 28-R obtained with the engine in flight as well as a comparison of fuel knock limits with engine cooling limits for the flight installation are given in part II (reference 2). A comparison of the knock-limited performance of the flight and the test-stand engines, with a grade 91/96 fuel, has been reported in preliminary form.

With a view toward making a fairly comprehensive comparison of the cooling characteristics of the two engine installations, similar cooling-correlation runs were made with both. Because both engines were equipped with the same instrumentation, insofar as location and methods of measurement of engine temperatures and cooling-air pressures were concerned, an excellent opportunity was afforded to correlate directly the cooling characteristics of flight and test-stand installations. The present report, part III in the series, presents a comparison of the two installations based on the method of correlating cooling characteristics developed in reference 3.

The development and analysis of the flight cooling data presented in this report follow the same procedure and are based on the same test runs used in the flight cooling correlation of reference 1. However, the two correlations differ in the following respects. The installation of the rear-spark-plug-boss thermo-couples, upon which the analysis presented herein is based, and the arrangement of cooling-air pressure tubes differ from those of

part I. These deviations from "standard" procedure were made in order that the cooling of the flight and test-stand engines could be compared using identical instrumentation. In order to show the fundamental relation between fuel-air ratio and mean effective gas temperature T_{g_0}, a large number of data from test runs covering a wide range of engine conditions, both for the flight and test-stand installations, are presented herein. In reference 1 only a limited number of runs with variable fuel-air ratio were shown that were taken at the time the flight cooling-correlation data were obtained.

EQUIPMENT AND INSTRUMENTATION

The flight engine (R-1830-90C) was mounted in the left inboard nacelle of a B-24D airplane. A view of this engine with propeller and cowling removed is shown in figure 1. The same model test-stand engine was installed in a test cell equipped to provide ground-level external-cooling and exhaust-pressure conditions; power was absorbed by a three-blade propeller (diam., 10 ft 6 in.). The test-stand engine was equipped with a cowling from a C-47A airplane.

All cylinder and induction-system thermocouples and cooling-air pressure tubes were installed in as nearly as possible the same positions for both engines. The installation of the rear-spark-plug-boss thermocouples used in this comparison was one that conformed to standard NACA cooling practice prior to March 1944. A thermocouple was inserted 1/8 inch into the head metal of the rear-spark-plug boss at the six o'clock position with respect to the spark-plug hole of all cylinders. The holes into which these thermocouples were peened were centered approximately 3/8 inch radially out from the edge of the threaded hole in the spark-plug bushing. Rear middle-barrel thermocouples (for all cylinders) were spot-welded to the cylinder outer surface between the sixth and seventh fins, counting from the uppermost barrel fin. The thermocouple locations on the cylinder are shown in figure 2. The rear middle-barrel thermocouple is designated T_6; the rear-spark-plug-boss thermocouple, T_{37}; and the rear-spark-plug-gasket thermocouple (flight engine only), T_{12}.

Cooling-air pressure tubes were installed according to standard NACA practice and were located as shown in figure 2. Each front-row cylinder head was provided with two total-pressure tubes and each front-row cylinder barrel was provided with a single total-pressure tube. One static-pressure tube was installed for each

rear-row cylinder head and each rear-row cylinder barrel. Although
the flight engine was equipped with a larger complement of tubes than
the test-stand engine, calculations for this report were based on
the reduced number that corresponded to those installed on the test-
stand engine. Data on cooling-air pressure drop were calculated
from averaged total pressures measured at the front-row cylinders
and averaged static pressures measured at the rear-row cylinders.

     Readings of individual cylinder-head pressure tubes around
the engine, both static and total, were averaged to obtain values
of average cylinder-head pressure drop. Similarly, readings of
individual cylinder-barrel pressure tubes around the engine were
averaged to obtain average cylinder-barrel pressure drop. All
reported values of cooling-air pressure drop were measured across
the entire engine and are therefore the total drop across both
the front and the rear rows of cylinders. Values of σ (ratio of
cooling-air stagnation density at face of engine to NACA standard
density at sea level) were computed from the total air pressure
at the face of the engine and the stagnation-air temperature. The
stagnation-air temperature was obtained from the measured free-air
temperature plus a computed adiabatic temperature rise due to
compression at the face of the engine.

     Carburetor-air temperatures were measured for both engines
by thermocouples attached to the carburetor screen and were read
from a potentiometer. Fuel-air ratios were determined by inde-
pendent measurements of fuel flow and air flow for both engines.
In flight, air flows were calculated from an air-box calibration
of the carburetor and suitable correction curves based on ground
air-flow tests with the carburetor installed in the airplane.
Test-stand air-flow measurements were obtained from a 6-inch,
square-edge orifice in the charge-air duct. Fuel flows for both
installations were obtained from rotameters. Additional checks on
fuel flow in flight were obtained by means of a deflecting-vane-
type flowmeter and a thermal flowmeter developed by the NACA.

PROCEDURE

     Test-stand cooling runs were made at ground-level atmospheric
conditions; flight tests were conducted during a single flight at
at a pressure altitude of 7000 feet. The general procedure for
establishing multicylinder-engine cooling characteristics by the
NACA method of correlation (developed in reference 3) was followed.

     The following is the correlation equation, which expresses
the effect of charge-air flow and cooling-air $\sigma \Delta p$ upon the
engine temperature level. (A complete derivation for this equation
is given in reference 3.)

$$\frac{T - T_a}{T_g - T} = K \cdot \frac{M_e{}^n}{(\sigma \Delta p)^m} \tag{1}$$

All the following quantities are measured directly except T_g, which is estimated from previous cooling experience.

T average engine temperature, either heads or barrels, $°F$

T_a cooling-air stagnation temperature, $°F$

T_g mean effective gas temperature, either heads or barrels, $°F$

M_e engine charge-air weight flow, pounds per hour

Δp average cooling-air pressure drop, inches of water

σ ratio of cooling-air stagnation density at face of engine to NACA standard density at sea level

The following quantities must be evaluated by the cooling runs:

n exponent through which M_e affects engine temperatures

m exponent through which $\sigma \Delta p$ affects engine temperatures

K an experimentally determined constant for a particular engine and installation

Three basic types of run are necessary to establish completely the cooling relations: variable charge-air flow, variable cooling-air pressure drop, and variable fuel-air ratio. All runs in which the cooling correlations were established were made at an engine speed of approximately 2230 rpm in low blower ratio with a spark advance of $25°$ B.T.C. Engine-temperature data for additional runs with variable fuel-air ratio at other engine speeds and both blower ratios are presented. Table I lists ranges of the primary variables for the two engines.

METHOD OF CALCULATION

The treatment of data followed, in general, the method set forth in reference 3 and applied in references 4 and 5. In such analyses, the following terms, additional to those just listed, are customarily employed:

T_h average cylinder-head temperature, $^\circ$F

T_{g_h} mean effective gas temperature for cylinder heads, $^\circ$F

T_{g0_h} mean effective gas temperature for cylinder heads of
         reference carburetor-air temperature of 0° F

ΔT_{g0_h} change in mean effective gas temperature for cylinder heads
         corresponding th variation in induction-system temper-
         atures (based on carburetor-air temperature of 0° F)

c   factor that accounts for effects of blower-gear ratio,
         impeller diameter, and thermodynamic process upon charge-
         air temperature rise through supercharger, (see refer-
         ences 4 and 5)

T_c carburetor-air temperature, $^\circ$F

N   engine speed, rpm

         Calculations of the quantity $\dfrac{T_h - T_a}{T_{g_h} - T_h}$ and a similar term

for cylinder barrels were based on an assumed mean effective gas
temperature for a given fuel-air ratio. This value for a
carburetor-air temperature of 80° F has been customarily assumed
to be 1150° F for cylinder heads and 600° F for cylinder barrels
at a fuel-air ratio of 0.08. (See reference 4.)

         During 1944 most NACA cooling-correlation work was done using
the parameter T_{g0} (reference carburetor-air temperature of 0° F)
instead of T_{g80} (carburetor-air temperature, 80° F). When this
procedure is followed, the assumed value of T_{g0} for cylinder
heads becomes 1086° F and for cylinder barrels, 536° F at a fuel-
air ratio of 0.08. The equation

$$\Delta T_{g0} = \left[T_c + c \left(\frac{N}{1000} \right)^2 \right] f \qquad (2)$$

expresses the change in the mean effective gas temperature caused
by variation in induction-system temperatures. The values of the
empirical factor f was 0.8 for heads and $0.8 \left(T_{gb} / T_{gh} \right)$, or 0.42,
for barrels, the development of equation (2) is given in refer-
ence 4. Because of the unavoidable variation in fuel-air ratio
experienced with the flight engine while making certain of the basic
correlation runs, it was necessary to adjust the assumed value of T_{g0}

for deviation from a fuel-air ratio of 0.08. This correction made use of a portion of a typical T_{g_O} curve established in test-stand work.

A typical calculation of the quantity $\dfrac{T_h - T_a}{T_{g_h} - T_h}$ follows. The data correspond to the highest-power flight run in which charge-air flow was the variable.

Charge-air flow M_e, pounds per hour/1000 . . . . 7.230
Fuel flow, pounds per hour. 635
Stagnation-air temperature T_a, $^\circ$F 54
Carburetor-air temperature T_c, $^\circ$F 75
Average rear-spark-plug-boss temperature T_h, $^\circ$F 411
Average rear middle-barrel temperature T_b, $^\circ$F 343
Engine speed N, rpm 2230

The fuel-air ratio obtained from the values of fuel and air flow is then

$$\frac{635}{7230} = 0.0878$$

From a portion of a typical $T_{g_{O_h}}$ curve passing through 1086° F at a fuel-air ratio of 0.08,

$$T_{g_{O_h}} = 1033^\circ \text{ F}$$

By substitution in equation (2)

$$\Delta T_{g_{O_h}} = \left[75 + 19.5 \left(\frac{2230}{1000} \right)^2 \right] 0.80$$

$$\Delta T_{g_{O_h}} = 138^\circ \text{ F}$$

By definition

$$T_{g_h} = T_{g_{O_h}} + \Delta T_{g_{O_h}} = 1033 + 138 = 1171^\circ \text{ F}$$

Therefore

$$\frac{T_h - T_a}{T_{g_h} - T_h} = \frac{411 - 54}{1171 - 411} = 0.470$$

A similar calculation is made for cylinder barrels using the value for average rear middle-barrel temperature (343° F), a portion

of a typical T_{g_0} curve for barrels obtained from test-stand data, and a factor of 0.42 in place of 0.80 for the calculation of ΔT_{g_0} for barrels.

The data for nine variable charge-air flow runs in flight, eight variable charge-air flow runs in the test stand, ten variable cooling-air $\sigma \Delta p$ runs in flight, and five variable cooling-air $\sigma \Delta p$ runs in the test stand were computed and are plotted as construction curves in figures 3 and 4. (Magnitude and range of the test variables are shown in table I for both engines.)

RESULTS AND DISCUSSION

Development of Cooling-Correlation Curves

The exponent n (equation (1)) through which charge-air flow M_e affects the functions $\dfrac{T_h - T_a}{T_{g_h} - T_h}$ and $\dfrac{T_b - T_a}{T_{g_b} - T_b}$ is evaluated from the slopes in the logarithmic construction plots of figure 3. The effect of charge-air flow upon these functions and, consequently, upon engine temperature level is seen to be greater for the flight engine than for the test-stand engine. This apparent difference in exponents for M_e between the two engines may be due in part to the fact that, for the flight engine, exhaust pressure increased to some extent as the engine manifold pressure was raised owing to use of the turbosupercharger. The exponent m through which cooling-air $\sigma \Delta p$ affects $\dfrac{T_h - T_a}{T_{g_h} - T_h}$ and $\dfrac{T_b - T_a}{T_{g_b} - T_b}$ is obtained from figure 4. The effect of $\sigma \Delta p$ upon the engine temperature level is greater for the flight engine than for the test-stand engine, for both heads and barrels; this difference may be partly attributed to the difference in design of the cowlings for the two engines.

From the experimentally determined exponents (slopes) of the construction plots in figures 3 and 4, correlation curves of the type shown in figure 5 may be drawn. If equation (1) is rearranged to permit plotting a logarithmic correlation curve having, for convenience, the same numerical slope as in figure 4,

$$\frac{T - T_a}{T_g - T} = K \left(\frac{M_e^{\,n/m}}{\sigma \Delta p} \right)^m$$

where m, the final exponent, is the slope of the correlation curve. The values of the combination exponent n/m used in plotting the final cooling-correlation curves (fig. 5) were as follows:

	Heads	Barrels
Test stand	1.88	1.52
Flight	1.96	1.71

Before the correlation curves could be plotted in final form, several series of preliminary plots of these lines had to be made to correct the initial construction lines to compensate for the unavoidable variation in cooling-air $\sigma\Delta p$ and engine charge-air flow. These variables, ideally, should have remained constant over a given set of runs but, owing to conditions difficult to control, were allowed to change somewhat. Three series of corrections were made to both the construction plots and the correlation lines before the error due to these variations was reduced to a negligible quantity.

The correlation lines in final form are presented in figure 5 for the test stand and for flight. The two sets of lines are shown on different areas of the grid inasmuch as the variation in exponents between flight and test stand may cause a difference in the position of the lines on a single grid, the interpretation of which can be misleading upon casual inspection. Any comparative analysis of the cooling characteristics of these engines must be arrived at either by substituting specific values of M_e, $\sigma\Delta p$, and the exponent n/m into the abscissas of the two plots (figs. 5(a) or (b))

in order to determine the functions $\dfrac{T_h - T_a}{T_{g_h} - T_h}$ and $\dfrac{T_b - T_a}{T_{g_b} - T_b}$ or by

algebraically solving the appropriate correlation equations that express the cooling characteristics of the two engines. These equations, defining the lines in figure 5, are as follows:

For heads:

(Test stand) $\dfrac{T_h - T_a}{T_{g_h} - T_h} = 0.300 \left(\dfrac{M_e^{1.88}}{\sigma\Delta p}\right)^{0.292} = 0.300 \left[\dfrac{M_e^{0.549}}{(\sigma\Delta p)^{0.292}}\right]$

(Flight) $\dfrac{T_h - T_a}{T_{g_h} - T_h} = 0.310 \left(\dfrac{M_e^{1.96}}{\sigma\Delta p}\right)^{0.312} = 0.310 \left[\dfrac{M_e^{0.612}}{(\sigma\Delta p)^{0.312}}\right]$

For barrels:

(Test stand) $\qquad \dfrac{T_b - T_a}{T_{g_b} - T_b} = 0.823 \left(\dfrac{M_e^{1.52}}{\sigma \Delta p}\right)^{0.391} = 0.823 \left[\dfrac{M_e^{0.594}}{(\sigma \Delta p)^{0.391}}\right]$

(Flight) $\qquad \dfrac{T_b - T_a}{T_{g_b} - T_b} = 0.797 \left(\dfrac{M_e^{1.71}}{\sigma \Delta p}\right)^{0.430} = 0.797 \left[\dfrac{M_e^{0.735}}{(\sigma \Delta p)^{0.430}}\right]$

An alternate method of plotting the correlation curves for the two engines affords a somewhat more direct comparison of the cooling characteristics. If a mean value of the exponent n/m is used for plotting correlation curves of both engines instead of the individual values for test stand and flight used in figure 5, the slopes and the position of these curves will be altered to some extent. This presentation, as shown in figure 6, permits a comparison of the cooling characteristics of the two engines to be made in the same area of a single graph. In figure 6 the two curves for heads are plotted against the same abscissa (horizontal scale) instead of against different scales, as was done, in effect, in figure 5; the same is true of the curves for barrels. The possible error in results obtained when temperatures are predicted using the cooling equations with averaged exponents (fig. 6), as compared with individual exponents (fig. 5), was generally found to lie within the experimental error of the original data. However, use of the individual equations or curves will result in a higher degree of accuracy than is available using the averaged values.

Effect of Fuel-Air Ratio on Mean Effective Gas Temperature T_{g_0}

Figure 7 shows the effect of fuel-air ratio upon the mean effective gas temperature T_{g_0} for both the test-stand and the flight engines. These curves facilitate the prediction of cooling characteristics for a wide range in mixture strength. In figure 7(a) are shown a large number of data, which serve to illustrate several features: (a) These data establish the shape of the curve of T_{g_0} against fuel-air ratio for these engines; (b) they demonstrate that, for the rather wide range of conditions covered by the test data for the two engines, both engine installations exhibit the same T_{g_0} curve and both show about the same band of scatter in the data; and (c), and of perhaps the greatest significance, these data demonstrate the successful reduction and correlation of a large volume of unrelated and widely varied data from

both engines. These data include tests under knocking and non-knocking conditions; data for 28-R, grade 91/96, and two high-performance fuels; and tests at several engine speeds, at both blower ratios, and with a number of carburetor-air temperatures. The faired curves in figure 7(b) were drawn as nearly as possible through the average of the test data while intersecting the initially assumed temperatures of 1086° and 536° F at a fuel-air ratio of 0.08.

Temperature Conversions

Graphs of maximum cylinder-head temperature against average (of 14 cylinders) are shown in figure 8(a) and (b) for the test-stand and flight engines, respectively. Similar relations for barrels are shown in figure 9(a) and (b). This information is necessary in order to apply cooling-correlation relations to a specific engine. Thus, if a calculation is to be based on some limiting engine temperature, that value will be considered as the maximum (of 14 cylinders) and must be converted to an average engine temperature to permit using the correlation plots and equations that are based on average temperatures. It will be noted in figure 8 that maximum head temperatures, both for test stand and for flight, tend to deviate farther from the average with increasing temperature; the flight engine shows, in general, the greater deviation. Maximum barrel temperatures, however, show more nearly a constant difference from the average throughout the temperature range than that for heads (fig. 9); this difference is greater for the flight engine.

Figures 10 and 11 are included as a further source of pertinent information to show the relations of maximum and average rear-spark-plug-gasket temperatures to average rear-spark-plug-boss temperatures treated in this cooling correlation. Although the manufacturer's specified temperature limits are based on a maximum rear-spark-plug-gasket temperature, a conversion may be made from these graphs first to average rear-spark-plug-gasket temperature (fig. 10) and then to average rear-spark-plug-boss temperature (fig. 11). These data for comparing the two types of thermocouple were obtained from the flight engine.

Results of Comparative Calculations

Based on the cooling equations previously listed for the individual engines, calculations were made to compare the cooling characteristics of the two engines. Four specified engine-power conditions were selected for these comparisons: take-off power,

100 percent normal-rated power, 64 percent cruise power (maximum cruise), and 41 percent cruise power (minimum brake specific fuel consumption). For each of these conditions, three types of comparison were made; the results are presented in table II. In comparison A, for assumed equal charge-air flow (equal power) and cooling-air $\sigma\Delta p$, temperature comparisons between engines were computed for both heads and barrels. In comparison B, for assumed equal charge-air flow and engine temperatures, $\sigma\Delta p$ comparisons between engines were calculated. In comparison C, for assumed equal engine temperatures and $\sigma\Delta p$, engine charge-air flow (power) comparisons were computed. Values of cooling-limited brake horsepower were based on a simple correction of the nominal brake horsepower for difference in temperature-limited air flow.

Values of charge-air flow used in comparisons A and B were determined from the specific operating instructions (reference 6) and from estimated specific air-flow relations. Values of cooling air $\sigma\Delta p$ used in comparisons A and C were estimated from average values obtained in flight. Limiting cylinder-head temperatures in comparisons B and C were calculated and corrected from the manufacturer's maximum specified head (rear-spark-plug-gasket) temperatures (reference 6) by means of the conversion curves presented in figures 10 and 11 for the flight engine. Limiting rear middle-barrel temperatures were based on an arbitrary maximum value of 350° F, which corresponds roughly to the manufacturer's specified temperature limit of 335° F at the rear hold-down flange of the cylinder (reference 6). A relation between average (of 14 cylinders) values for these two temperatures is shown in figure 12 for the test-stand engine.

Table II lists all assumed conditions, parameters, and results for the comparative calculations. Under all power conditions and for each of the three types of comparison made, the flight engine (both heads and barrels) is seen to be the more critical with respect to cooling than the test-stand engine. This effect is apparent from the temperature difference (comparison A), the cooling-air $\sigma\Delta p$ difference (comparison B), and the temperature-limited air flow (and power) difference (comparison C). It is obvious, from the unreasonable results obtained in parts B and C for the assumed cylinder-barrel temperature limit, that a maximum barrel temperature of 350° F will be exceeded in flight, especially at the higher powers. This conclusion is substantiated by actual temperatures observed on the flight test engine during conventional operations, such as take-off, climb, and landing approach when maximum rear middle-barrel temperatures between 390° and 420° F were frequently observed. (See reference 2.) This temperature would also be exceeded by the test-stand engine at take-off conditions.

A graphical presentation of the temperature data in table II, comparison A, is given in figure 13. Only maximum values of predicted head and barrel temperatures are shown in this graph. One additional set of data not presented in table II is plotted in figure 13 - predicted values of maximum rear-spark-plug-gasket temperature for the flight engine. These data were obtained from the cooling-correlation predictions (average rear-spark-plug-boss temperature) in combination with the temperature conversions given in figures 10 and 11. From figure 13, head-temperature limits appear to be satisfactorily met by both engines at cruising and normal-rated power conditions. For take-off power the head-temperature limit is almost exceeded by the flight engine, but a considerable margin exists for the test-stand engine.

If the predicted maximum rear-spark-plug-gasket and rear middle-barrel temperatures for the flight engine in figure 13 are compared with the values predicted in table I of reference 1 for similar engine conditions, some difference in results will be noted, particularly for the cruising powers. This variation is mainly attributable to the difference in the curves of T_{g_0} against fuel-air ratio. The predicted temperatures in the present report are believed to be the more accurate because the T_{g_0} curve used herein (fig. 7) represents the averaged results of a much larger amount of test data than that used in reference 1.

SUMMARY OF RESULTS

The following results and cooling predictions are based on cooling tests conducted with two 14-cylinder double-row radial air-cooled engines, equipped as nearly as possible with the same instrumentation, one in a test stand and one in flight. These tests were made for both engines at an engine speed of approximately 2230 rpm, at low blower ratio, and with a spark advance of 25° B.T.C.

1. For the same operating and cooling conditions with both engines the test-stand engine was found, under all conditions, to run cooler than the flight engine (both cylinder heads and barrels).

2. The effect both of charge-air flow and of cooling-air pressure drop upon the heat-transfer processes for cylinder heads and barrels was somewhat greater for the flight engine than for the test-stand engine.

3. The reduction and correlation of a considerable amount of test data at widely varied engine conditions indicates that, within the scatter of the values for mean effective gas temperature T_{g_0},

the cooling characteristics of both engines are influenced by the same relation between T_{g_0} and fuel-air ratio.

4. Estimates of temperature-limited engine performance, based on cooling-air pressure drops experienced with the airplane, indicate that a maximum rear middle-barrel temperature of 350° F, which corresponds approximately to the manufacturer's specified temperature limit of 335° F at the rear hold-down flange of the cylinder, will be considerably exceeded by both engines at take-off power. At lower power levels, it appears that this temperature limitation will be exceeded by the flight engine at all the conditions investigated and may be exceeded by the test-stand engine at some conditions.

5. Both engines may be expected to satisfy temperature limits specified by the engine manufacturer for the rear spark-plug gasket at various rated-power conditions.

Aircraft Engine Research Laboratory,
        National Advisory Committee for Aeronautics,
            Cleveland, Ohio, February 23, 1945.

REFERENCES

1. Blackman, Calvin C., White, H. Jack, and Pragliola, Philip C.:
    Flight and Test-Stand Investigation of High-Performance Fuels
    in Double-Row Radial Air-Cooled Engines. I - Determination of
    the Cooling Characteristics of the Flight Engine. NACA MR
    No. E4L20, 1944.

2. White, H. Jack, Blackman, Calvin C., and Werner, Milton: Flight
    and Test-Stand Investigation of High-Performance Fuels in Double-
    Row Radial Air-Cooled Engines. II - Flight Knock Data and Com-
    parison of Fuel Knock Limits with Engine Cooling Limits in Flight.
    NACA MR No. E4L30, 1944.

3. Pinkel, Benjamin: Heat-Transfer Processes in Air-Cooled Engine
    Cylinders. NACA Rep. No. 612, 1938.

4. Corson, Blake W., Jr., and McLellan, Charles H.: Cooling Charac-
    teristics of a Pratt & Whitney R-2800 Engine Installed in an
    NACA Short-Nose High-Inlet-Velocity Cowling. NACA ACR No. L4F06,
    1944.

5. Morgan, James E., Bell, E. Barton, and Hill, E. John: Flight
      Investigation of the Altitude Cooling Characteristics of a
      Pratt & Whitney R-2800-5 Engine in a B-26B Airplane. NACA
      Memo. rep., Army Air Forces, Nov. 10, 1943. (Available as
      TN No. 1092, 1946.)

6. Anon: Operators Handbook (Part No. 51548). Twin Wasp C4 Engine.
      Pratt & Whitney Aircraft, 3d ed., March 1942.

TABLE I

RANGES OF PRIMARY VARIABLES IN COOLING-CORRELATION RUNS

Variable	Total number of runs		Range of variation	
	Test stand	Flight	Test stand	Flight
Charge-air flow, lb/hr	8	9	3000-6000	3610-7230
Manifold pressure, in. Hg abs.			23-40	25-48
Cooling-air $\sigma \Delta p$, in. H_2O:				
Barrels	5	10	11.1-23.5	4.2-15.4
Heads			11.5-24.7	4.8-17.2
Fuel-air ratio	112	74	0.053-0.110	0.054-0.113

TABLE II - COOLING COMPARISONS OF DOUBLE-ROW RADIAL AIR-COOLED ENGINES

IN A TEST STAND AND IN FLIGHT

(a) Specified Operating Conditions and Parameters for Comparative Calculations

Variable ↓ / Specified power condition →	Take-off	100 percent normal rated	64 percent (max.) cruise	41 percent cruise
Specified nominal operating conditions				
Engine speed, rpm	2700	2550	2250	1500
Manifold pressure, in. Hg absolute	48	41	28	30.5
Brake horsepower	1200	1100	700	450
Mixture-control setting	Auto-rich	Auto-rich	Auto-lean	Auto-lean
Maximum rear-spark-plug-gasket temperature, °F	500	450	450	450
Parameters for comparative calculations				
I Estimated charge-air flow, lb/hr	8500	6700	3900	3100
II F/A from carburetor	.097	.095	.065	.069
III Cooling-air $\sigma \Delta p$[1], heads, in. H_2O	8.3	11.3	6.7	4.6
IV Cooling-air $\sigma \Delta p$[1], barrels, in. H_2O	7.0	10.0	5.4	3.4
V Average rear-spark-plug-boss temperature[2], °F	494	444	444	444

[1] Estimated values corresponding to respective flight conditions for   engines installed in   airplane; cowl flaps one-third to one-fourth open for take-off and normal-rated power, closed for cruising.

[2] Values corresponding to nominal maximum rear-spark-plug-gasket temperature listed under specified operating conditions.

(b) Comparative Calculations for Temperature, Cooling-Air $\sigma \Delta p$, and Charge-Air Flow and Power

[Comparisons based on following assumed air conditions — take-off: cooling-air and carburetor-air temperatures, 100° F, ground-level σ; all other conditions: cooling-air and carburetor-air temperatures, 60° F; σ, approx. that for 7000-ft density altitude.]

Variable ↓ / Power condition and engine →	Take-off Test stand	Take-off Flight	100 percent normal rated Test stand	100 percent normal rated Flight	64 percent (max.) cruise Test stand	64 percent (max.) cruise Flight	41 percent cruise Test stand	41 percent cruise Flight
Comparison A (temperature)								
Average boss temperature, °F (assume I, II, and III)	462	492	376	400	376	395	362	379
Maximum boss temperature, °F	503	552	406	438	406	431	390	411
Average barrel temperature, °F (assume I, II, and IV)	384	406	321	340	331	340	325	336
Maximum barrel temperature, °F	415	452	346	384	357	384	351	380
Comparison B (cooling-air $\sigma \Delta p$)								
Average head $\sigma \Delta p$, in. H_2O (assume I, II, and V)	5.5	8.4	4.4	6.5	2.7	3.7	1.5	2.0
Average barrel $\sigma \Delta p$, in. H_2O (assume I, II, and 350° F maximum barrel temperature)	24.4	47.4	9.5	18.3	5.7	9.5	3.5	5.6
Comparison C (charge-air flow and power)								
(a) Charge-air flow (head-temperature limit), lb/hr (assume II, III, and V)	10,600	8400	11,100	8900	6400	5300	5700	4700
(b) Charge-air flow (barrel-temperature limit), lb/hr (assume II, III, 350° F)	3700	2760	6900	4700	3800	2800	3050	2310
Brake horsepower, estimated from (a)	1500	1190	1820	1460	1150	950	830	680
Brake horsepower, estimated from (b)	520	390	1130	770	670	500	440	340

NATIONAL ADVISORY
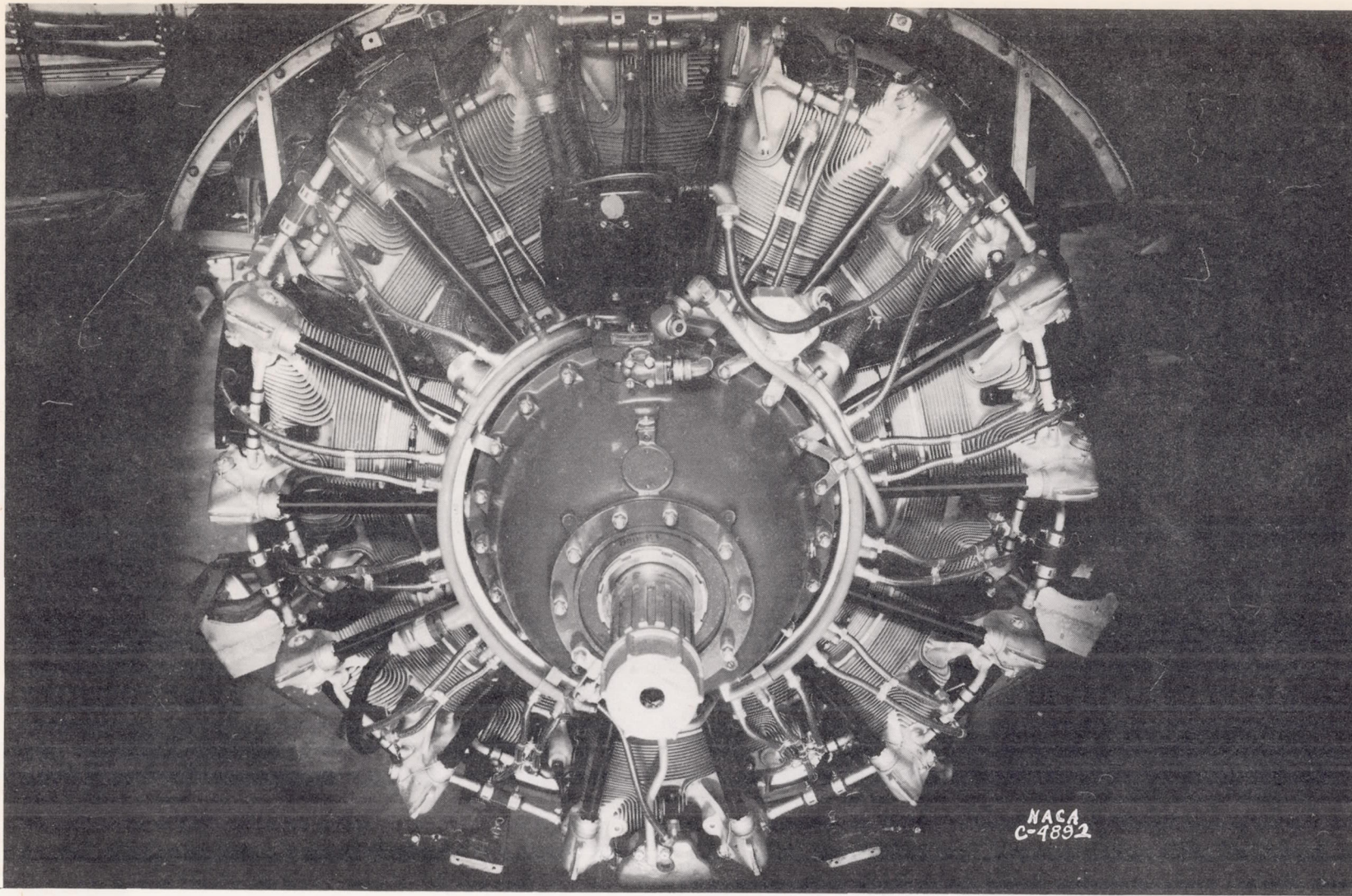COMMITTEE FOR AERONAUTICS

Figure 1. - Double-row radial air-cooled engine installed in four-engine airplane. Propeller, cowling, knock pickups, and leads removed.

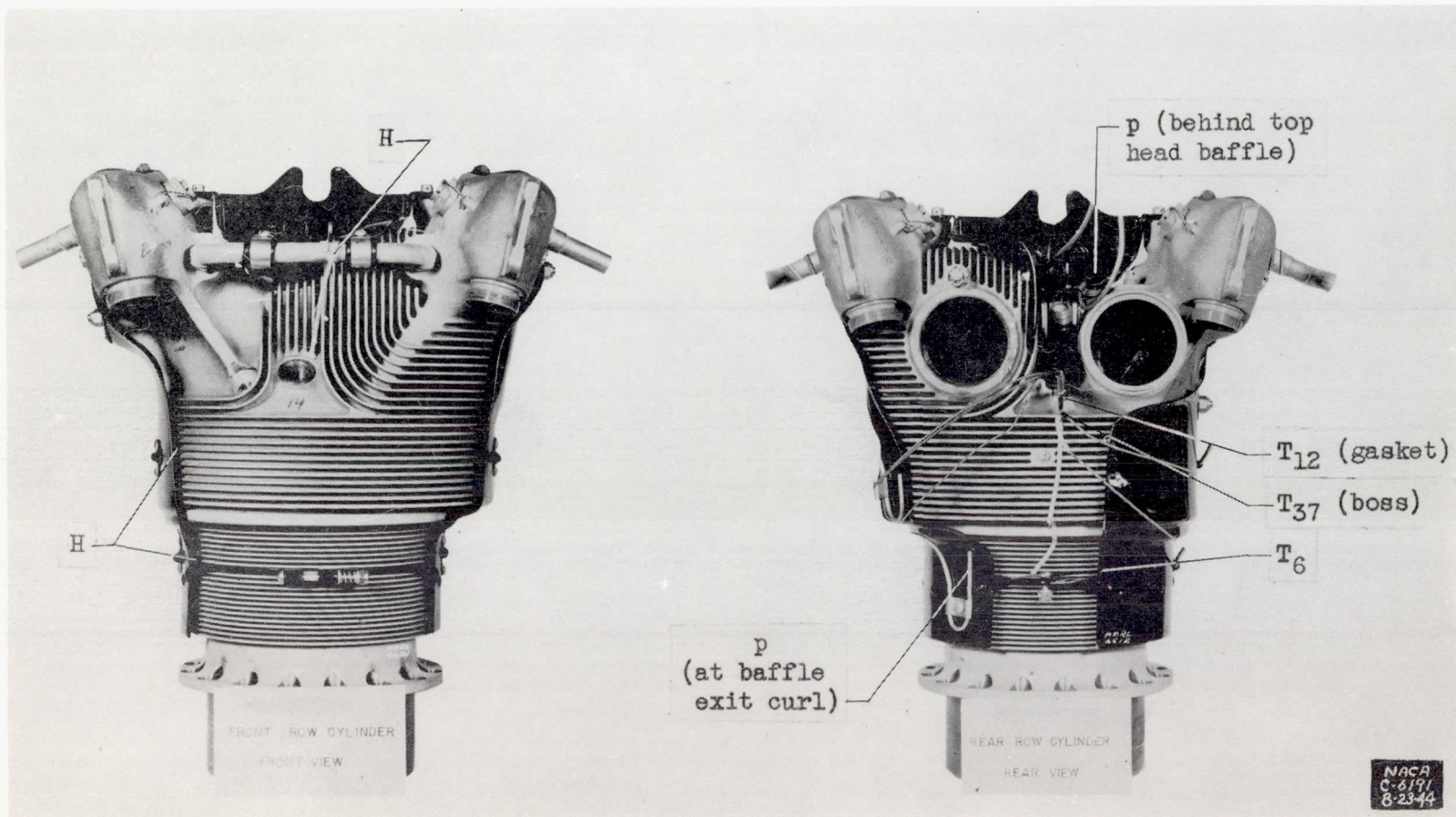Figure 2. - Typical installation of total-pressure tubes H, static-pressure tubes p, and thermocouples T used on air-cooled cylinders.
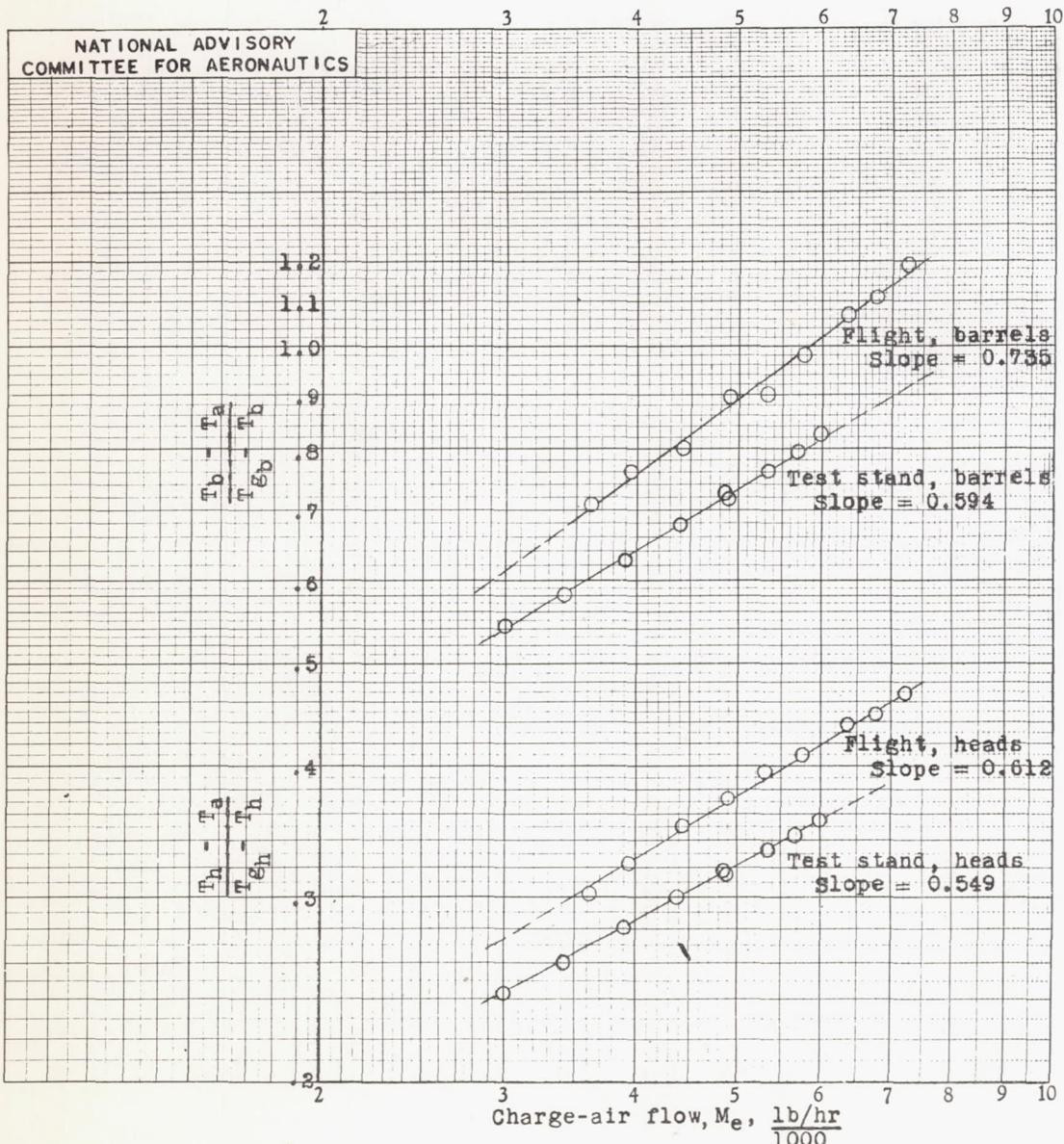
E-253

NATIONAL ADVISORY
COMMITTEE FOR AERONAUTICS

Flight, barrels
Slope = 0.735

Test stand, barrels
Slope = 0.594

Flight, heads
Slope = 0.612

Test stand, heads
Slope = 0.549

Charge-air flow, M_e, $\dfrac{lb/hr}{1000}$

Figure 3. - Variation of $\dfrac{T_h - T_a}{T_{g_h} - T_h}$ and $\dfrac{T_b - T_a}{T_{g_b} - T_b}$ with charge-air flow M_e for

double-row radial air-cooled engines in test stand and in flight. Engine
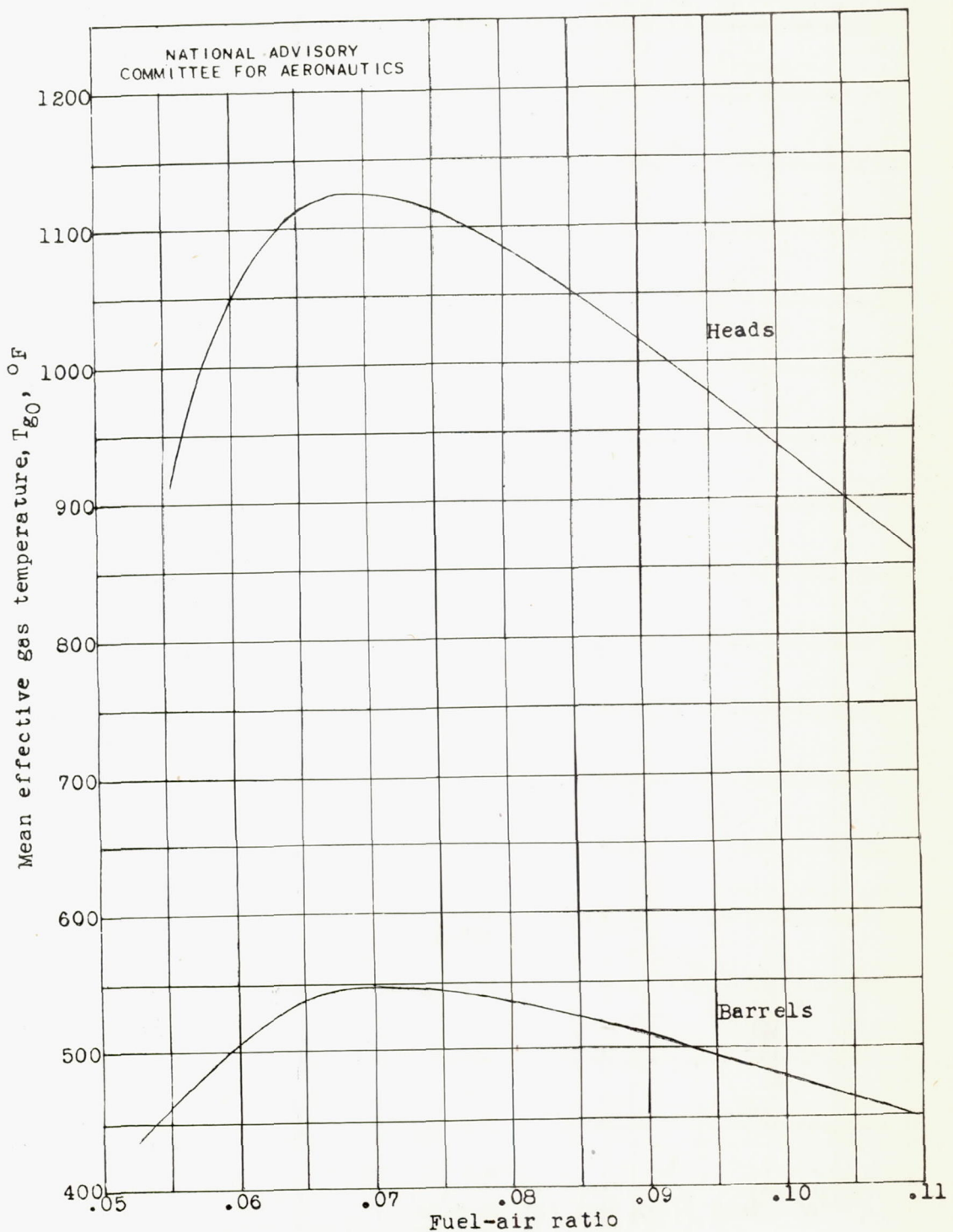speed, 2230 rpm; spark advance, 25° B.T.C.; low blower ratio.
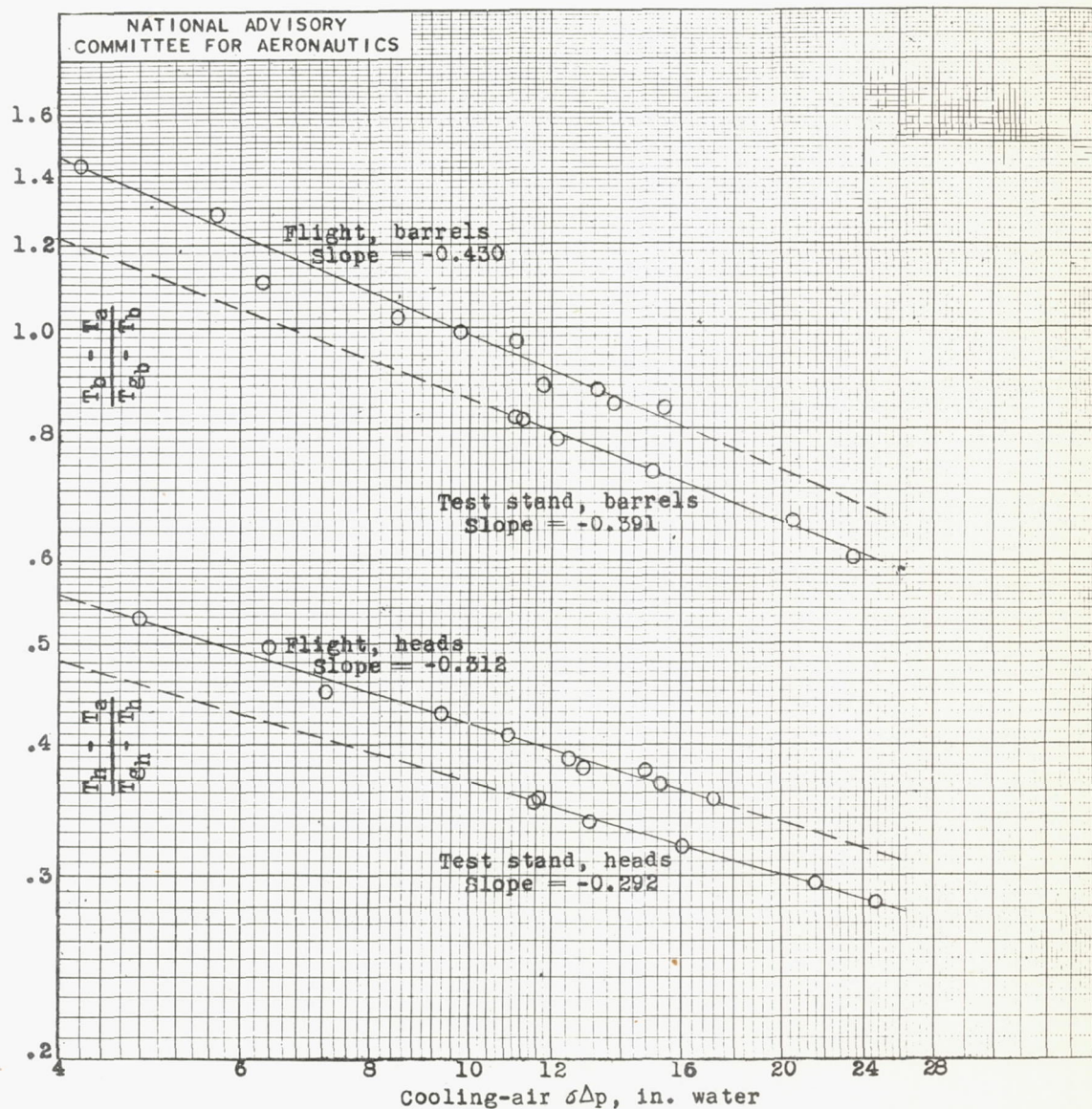
Figure 4. - Variation of $\frac{T_h - T_a}{T_{g_h} - T_h}$ and $\frac{T_b - T_a}{T_{g_b} - T_b}$ with cooling-air $\sigma\Delta p$ for double-row radial air-cooled engines in test stand and in flight. Engine speed, 2230 rpm; spark advance, 25° B.T.C.; low blower ratio.

E-253
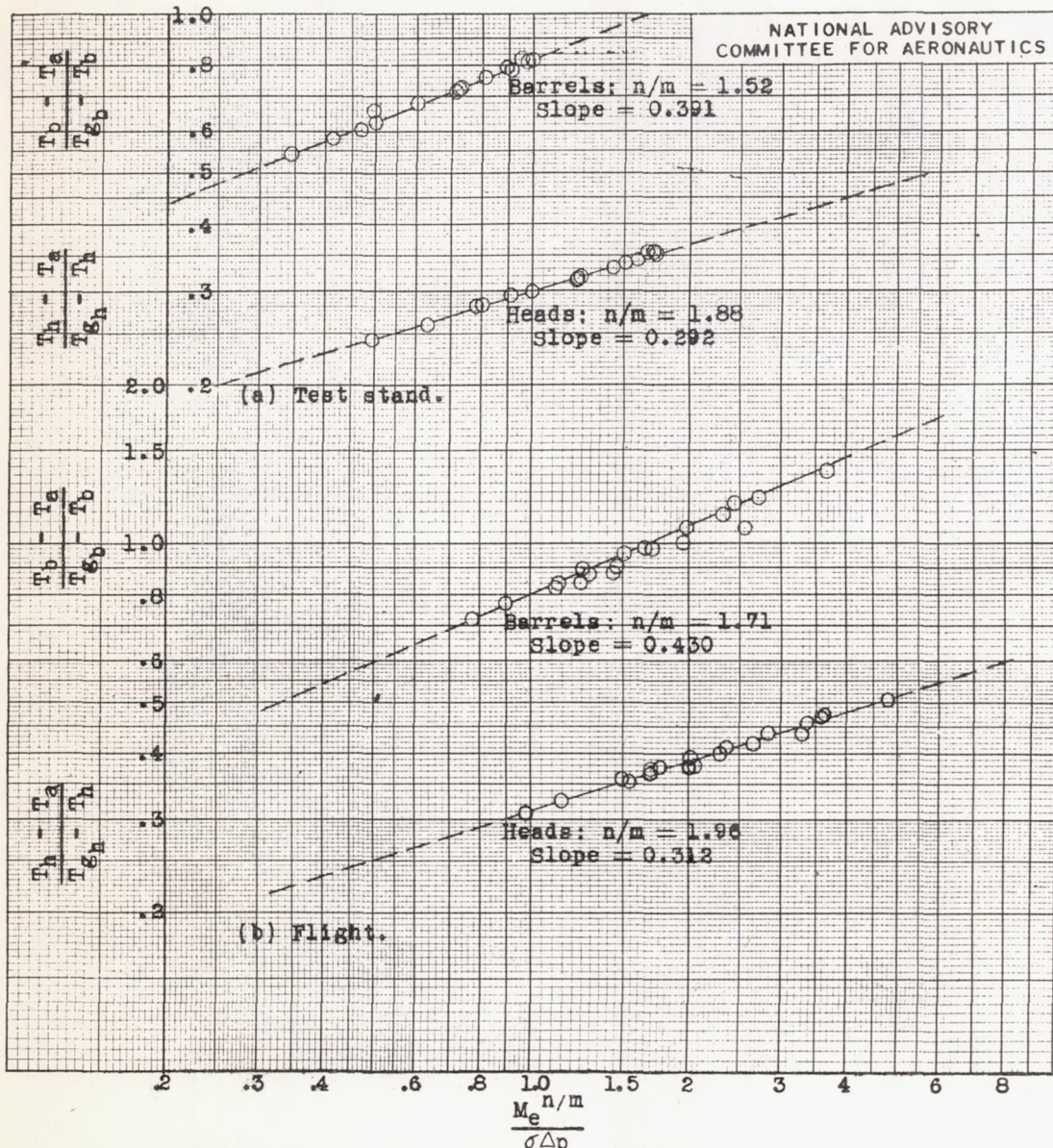
Figure 5. - Cooling-correlation curves for double-row radial air-cooled
engines in test stand and in flight. Engine speed, 2230 rpm; spark advance,
25° B.T.C.; low blower ratio.
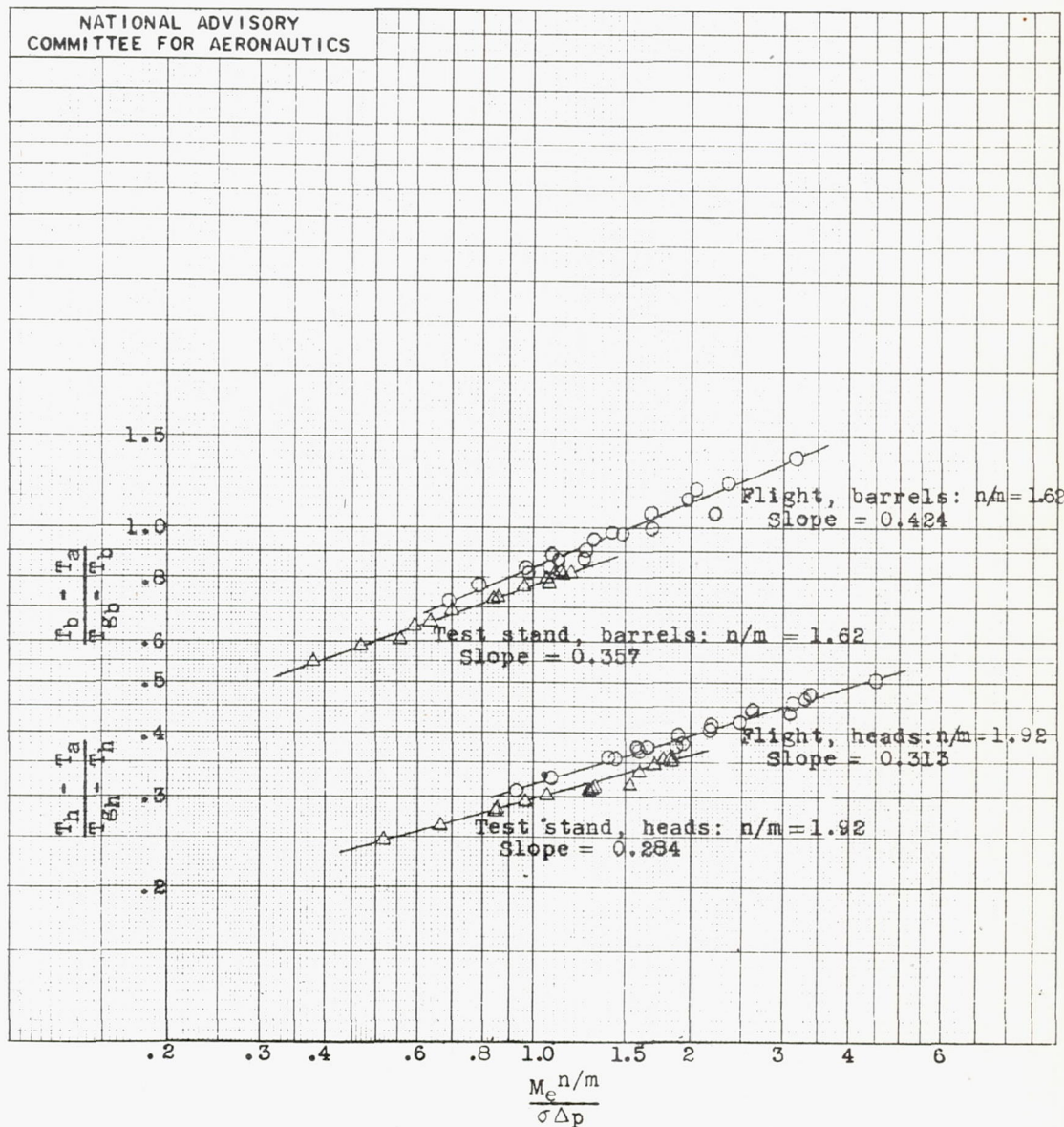
Figure 6. - Cooling-correlation curves for double-row radial air-cooled engines in test stand and in flight. Exponents n/m are averaged from individual values for each engine. Engine speed, 2230 rpm; spark advance, 25° B.T.C.; low blower ratio.

NATIONAL ADVISORY
COMMITTEE FOR AERONAUTICS

Heads

○ Test stand
△ Flight

Barrels

Mean effective gas temperature, T_{g_0}, °F
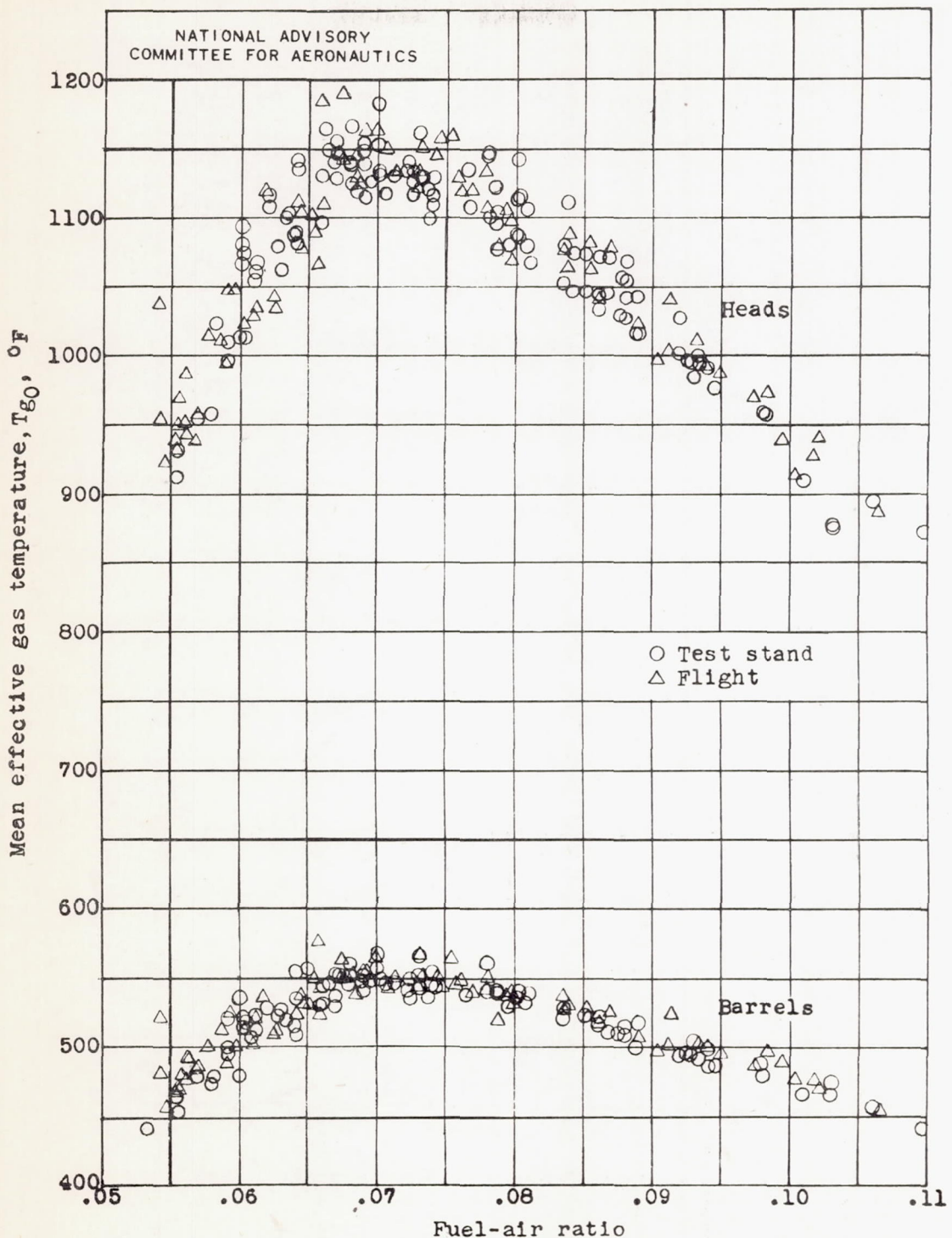
Fuel-air ratio

(a)   Test stand and flight data.

Figure 7. - Variation of mean effective gas temperature T_{g_0} with

fuel-air ratio for double-row radial air-cooled engines in a test
stand and in flight. Engine speed, 1800 to 2300 rpm; spark advance,
25° B.T.C.; high and low blower ratio; carburetor-air temperature,
80° to 150° F; data for four fuels under knocking and nonknocking
conditions.

(b) Faired curves for data in figure 7(a).

Figure 7. - Concluded.

E-253

NATIONAL ADVISORY
COMMITTEE FOR AERONAUTICS

O Variable charge-air flow
△ Variable cooling-air pressure drop

Maximum rear-spark-plug-boss temperature, °F

Average rear-spark-plug-boss temperature, °F
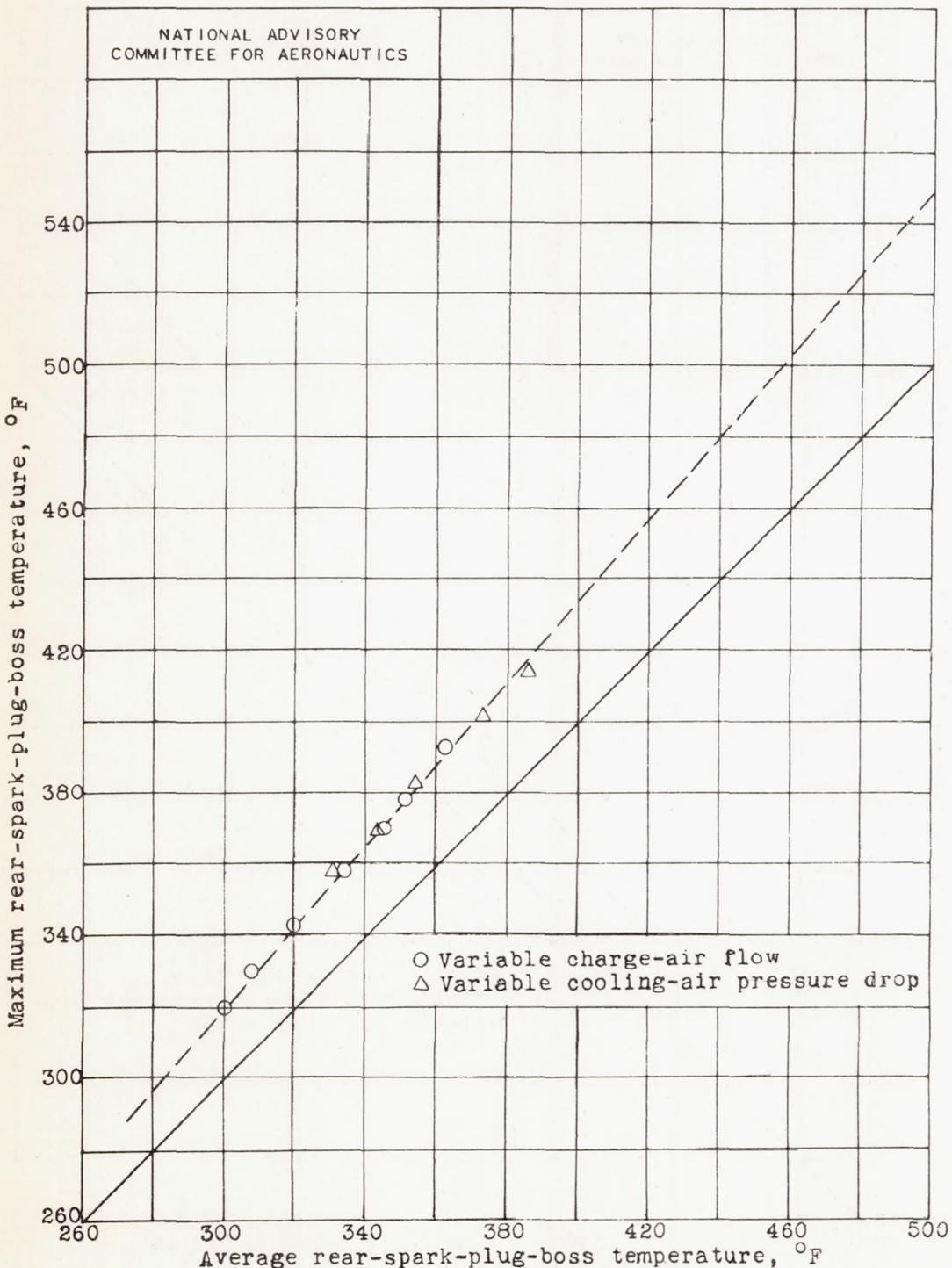
(a) Test stand.

Figure 8. - Variation of maximum with average rear-spark-plug-boss
     temperature for double-row radial air-cooled engine. Engine speed,
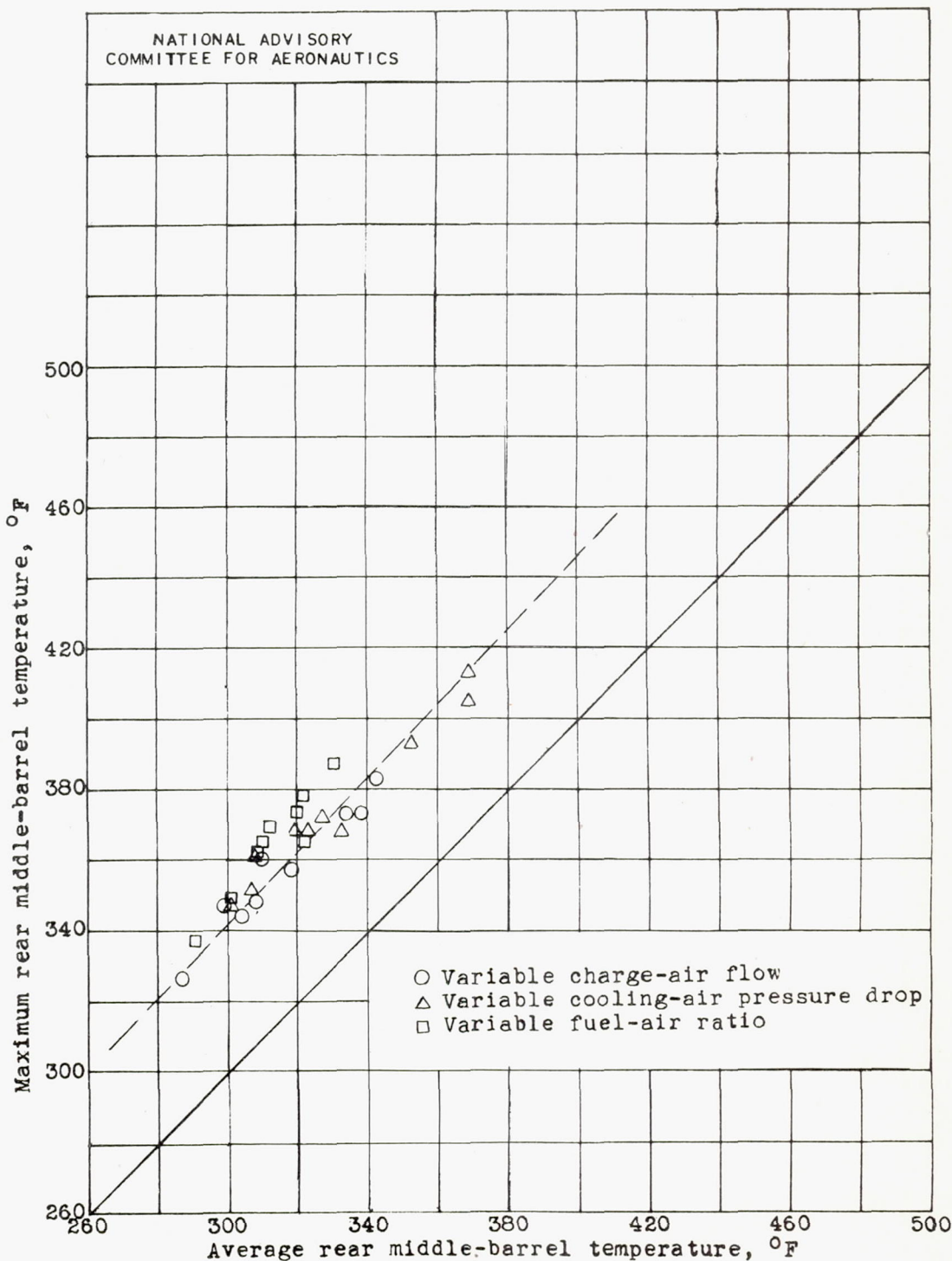   2230 rpm; spark advance, 25° B.T.C.; low blower ratio.
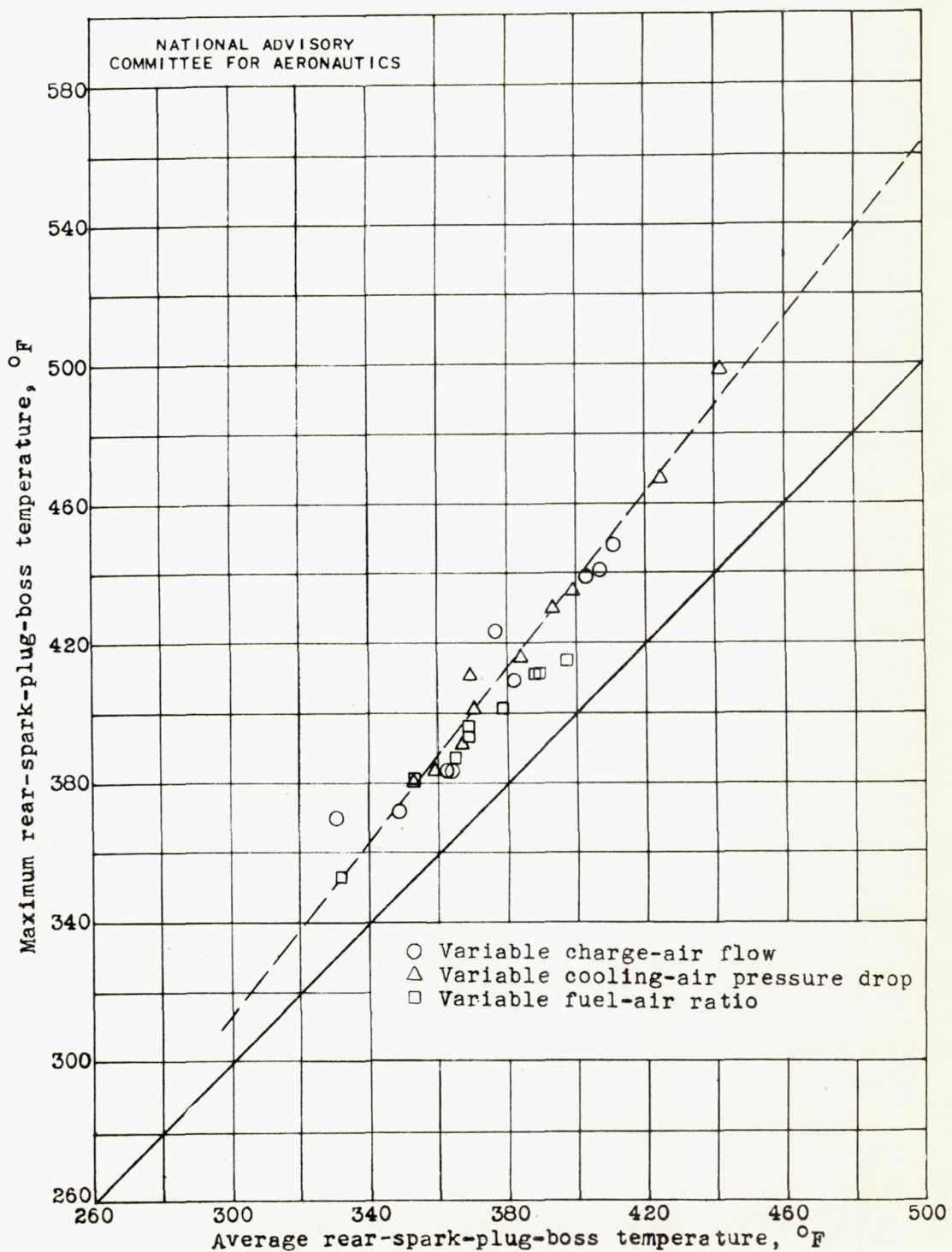
(b) Flight.
Figure 8. - Concluded.

E-253
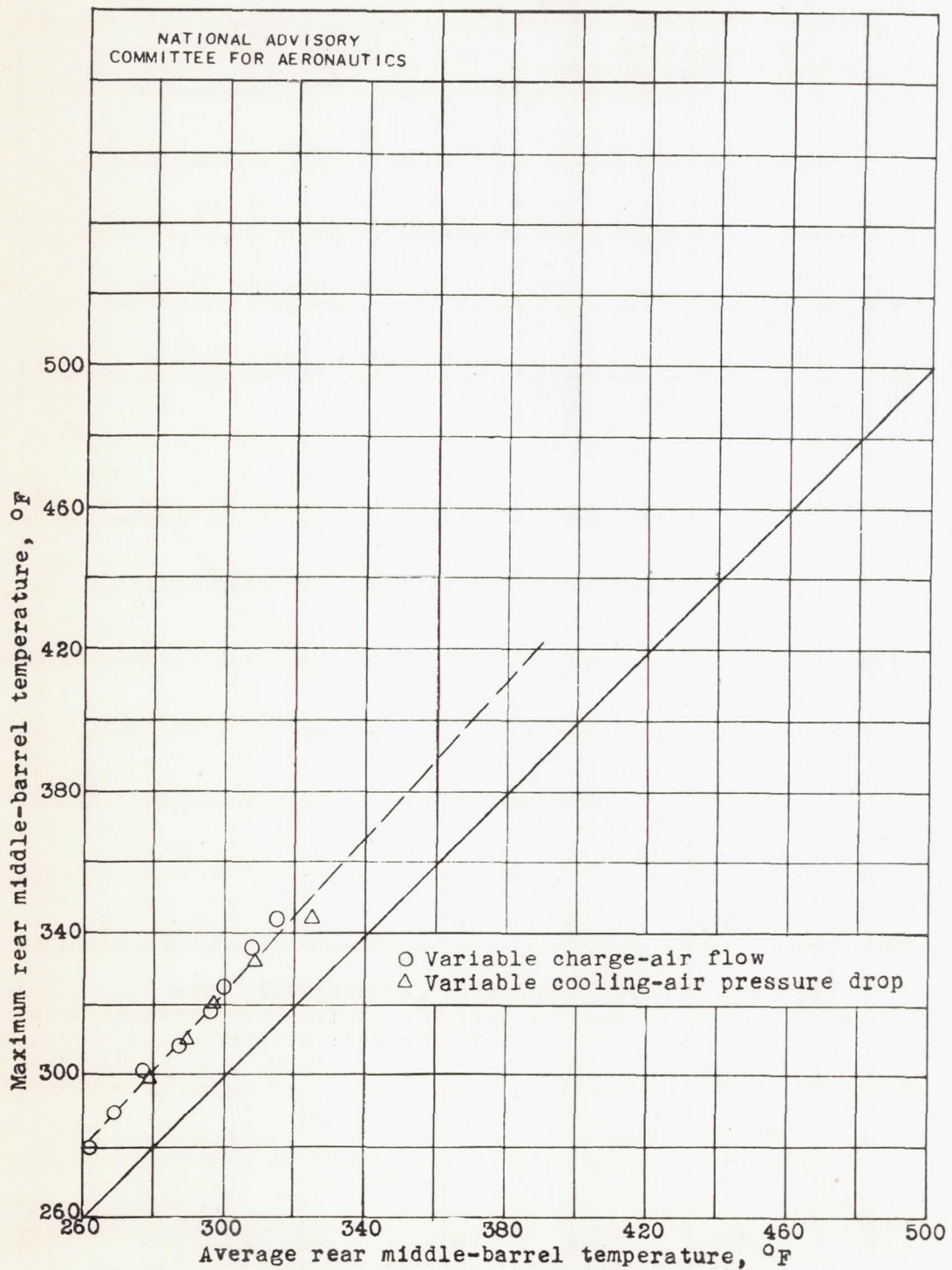
(a) Test stand.

Figure 9. - Variation of maximum with average rear middle-barrel
temperature for double-row radial air-cooled engine. Engine speed,
2230 rpm; spark advance, 25° B.T.C.; low blower ratio.

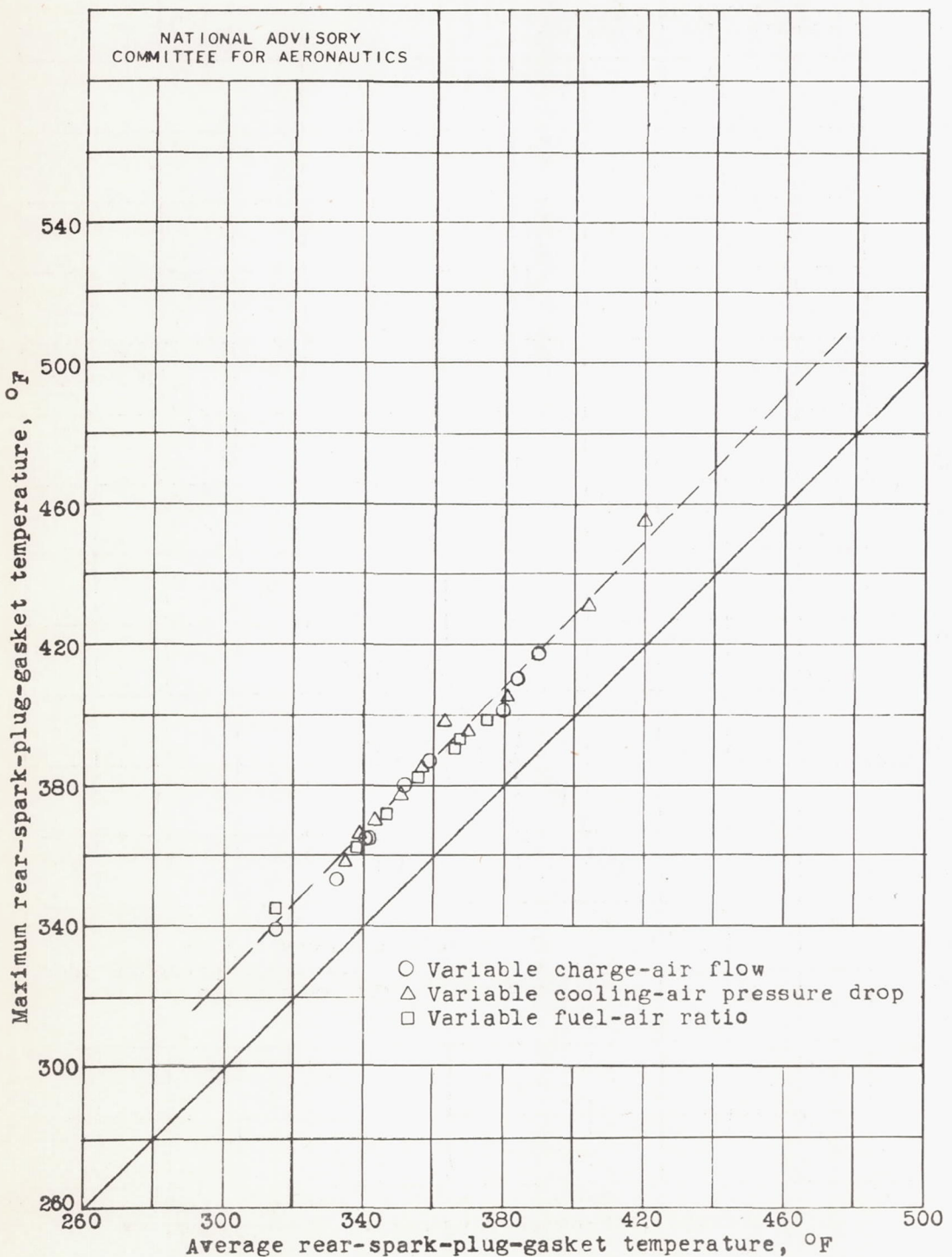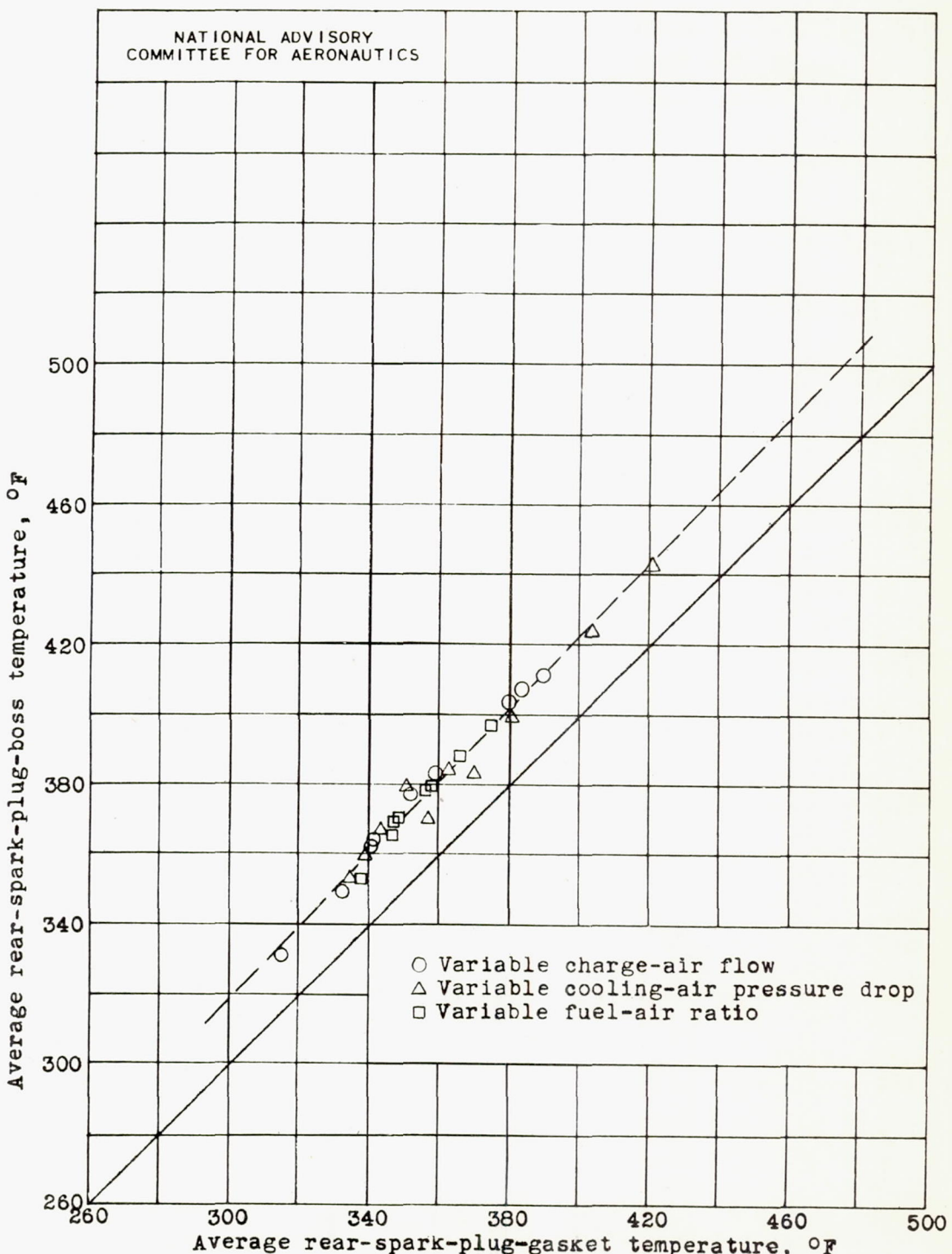(b) Flight.

Figure 9. - Concluded.

E-253

Figure 10. - Variation of maximum with average rear-spark-plug-gasket
temperature for double-row radial air-cooled engine in flight.
Engine speed, 2230 rpm; spark advance, 25° B.T.C.; low blower ratio.

Figure 11. - Comparison of average rear-spark-plug-boss temperature with average rear-spark-plug-gasket temperature for double-row radial air-cooled engine in flight. Engine speed, 2230 rpm; spark advance, 25° B.T.C.; low blower ratio.
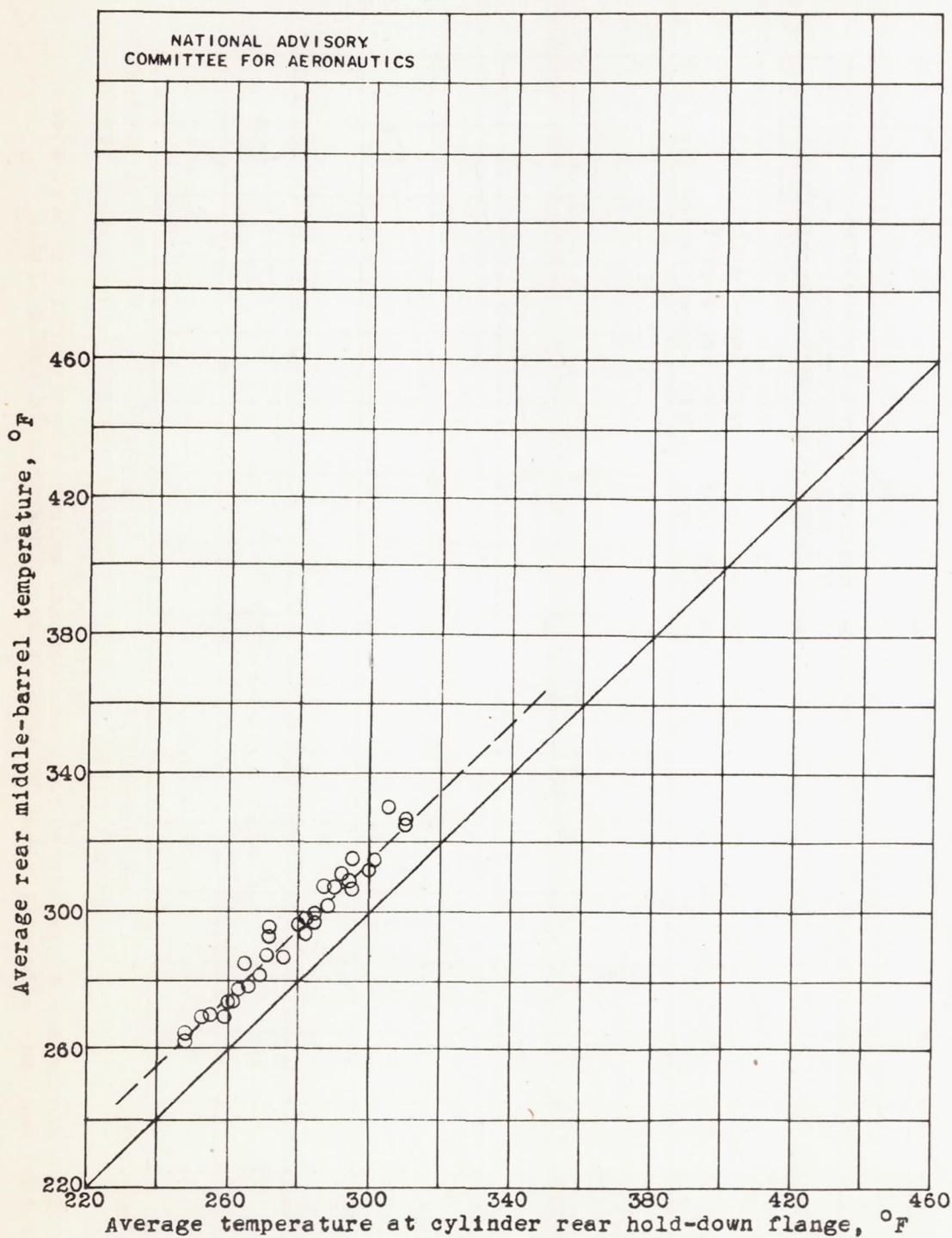
NACA MR No. E5B23

E-253

Figure 12. - Comparison of average rear middle-barrel temperature with average temperature at cylinder rear hold-down flange for double-row radial air-cooled engine in test stand. Engine speed, 2230 rpm; spark advance, 25° B.T.C.; low blower ratio.
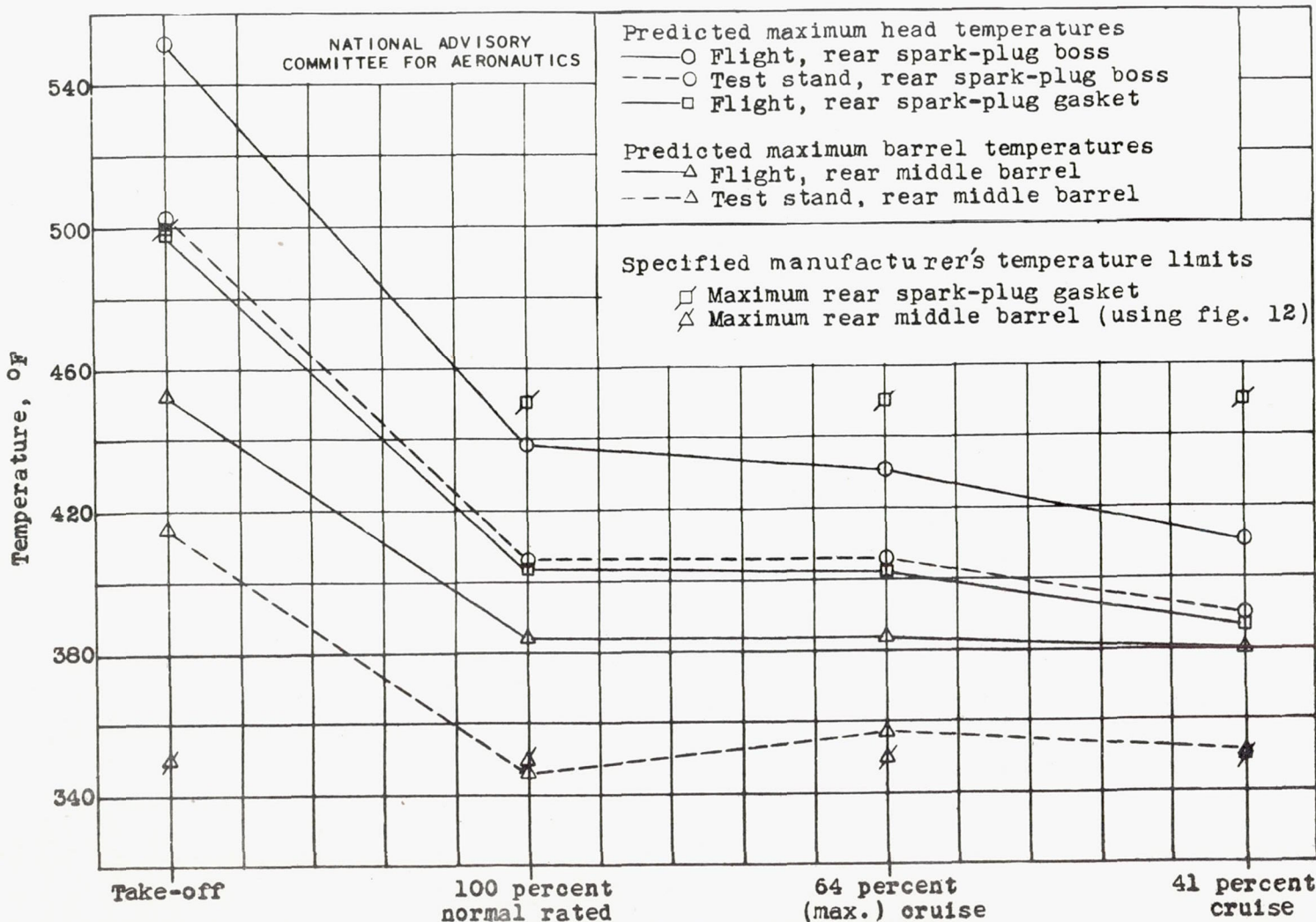
Figure 13. - Comparison of predicted maximum head and barrel temperatures for test stand and flight engines. Data correspond to temperature comparison in table II(a).

E-253